ELSEVIER

Journal of Nuclear Materials 294 (2001) 175–178

journal of nuclear materials

www.elsevier.nl/locate/jnucmat

Application of a new thermochemical measurement method for nuclear materials at temperatures beyond 3000 K

J.W. Hastie *, D.W. Bonnell, P.K. Schenck

Materials Science and Engineering Laboratory, NIST, Gaithersburg, MD, USA

Abstract

In processing and end-use environments, and particularly nuclear fission reactor excursions, inorganic materials can be subjected to temperatures where liquids and vapors are significant components of the materials system. Classical characterization and thermochemical methods fail at temperatures beyond about 3000 K, due to the reactivity of container materials. Use of a pulsed laser beam as a localized heat source avoids this limitation. Coupling laser heating with molecular beam sampling and mass- and optical-spectroscopy allows us to characterize the thermochemistry of liquid–vapor systems at temperatures of 3000–5000 K, pressures of 0.01–20 bar (1 bar = 10^5 Nm^{-2}), and on a nanosecond order-of-magnitude time scale. Materials considered here include C, ZrO_2, Y_2O_3 and HfO_2. New approaches for temperature measurement and for pressure determination, using electron impact mass spectral data coupled with deposition rate measurements, are described. © 2001 Published by Elsevier Science B.V.

1. Introduction

Since the development of nuclear fission reactors, the thermodynamic vaporization properties of nuclear materials have been key to model predictions and risk assessments of reactor excursions that attain very high temperatures. Accordingly, over the past two decades, considerable attention has been given to developing experimental methods that extend classical high temperature approaches to regions of higher temperatures and pressures. Table 1 summarizes the main efforts in this regard. In the present work, earlier limitations in quantifying temperature, pressure, and species concentrations have been essentially resolved, and representative data have been obtained on liquid oxide, carbide, and nitride refractories up to, and beyond their boiling points.

2. Approach

The basic approach utilizes a short pulse (7–30 ns) laser as a spatially ($\lesssim$1 mm^2) and temporally ($\lesssim$25 ns) confined heat source. The laser fluence (typically $\sim$1 J cm^{-2}) is adjusted to be, at the lower limit, just above the threshold for detectable vaporization and, at the upper limit, just below the threshold for formation of a visible laser-coupled plasma. Thus, a pulsed source of vapor is generated for in situ time-resolved mass spectral analysis. Velocity distribution analysis of the pulses provides valuable information on species thermal equilibration, temperature, gas dynamic history, and mass spectral electron impact processes, as discussed elsewhere [5]. Fig. 1 shows a schematic of the apparatus. Partial pressures (P_i) are obtained from

$$P_i = k_i I_i T_s, \tag{1}$$

where k_i is a constant based on system geometry and ionization characteristics, I_i is the observed mass spectral ion intensity, and T_s is the hot spot temperature at the target. The constant k_i is obtained from a pressure measurement based on deposition (and hence vaporization) rate measurements, taking into account the forward-peaked spatial distribution resulting from hydrodynamic flow [6].

Determination of total pressure (P_t) from deposition rate is well known for Knudsen effusion conditions. However, to our knowledge, this approach has not

* Corresponding author. Tel.: +1-301 975 5754; fax: +1-301 975 5335.

E-mail address: john.hastie@nist.gov (J.W. Hastie).

0022-3115/01/$ - see front matter © 2001 Published by Elsevier Science B.V.
PII: S0022-3115(01)00448-2

Table 1
Laser mass spectrometry approaches to species vaporization thermochemistry at very high temperatures

Approach	Year	Result	References
Long pulse IR laser	1985	UO_2, *P*s calibrated with literature data	Ohse et al. [1]
Long pulse IR laser	1988	UO_2, ZrO_2, cluster interference	Olander et al. [2]
Short pulse visible laser	1984, 1995	C, BN, temperature via indirect means	Hastie et al. [3,5]
Short pulse Nd/YAG laser	1996	UO_2, same approach as [3]	Joseph et al. [4]
Short pulse Nd/YAG laser at 1064 or 532 nm	Present	C, Al_2O_3, ZrO_2,Y_2O_3, HfO_2, direct T, P measurements, 3000–5500 K, 0.01–20 bar	This work and [6]

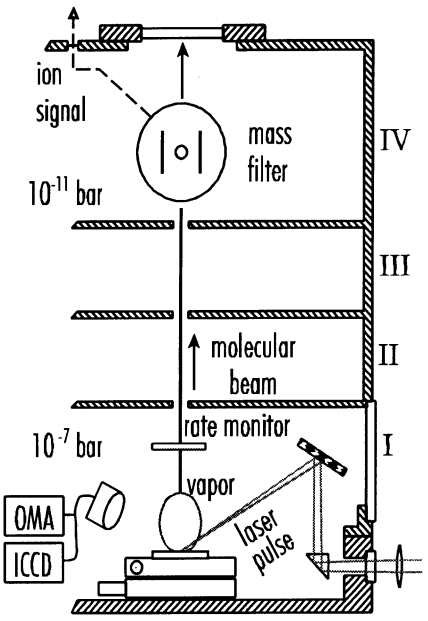

Fig. 1. Schematic of apparatus, including in situ deposition rate monitor, and optical multichannel analyzer (OMA) and intensified charge-coupled device (ICCD) optical detectors for temperature monitoring.

previously been used under hydrodynamic flow conditions, for which we derive the following relationship:

$$P_t = 10^{-6}\left(\frac{R(\ell^2+r^2)\pi\rho}{f\Delta t A}\left[\frac{2\pi R_g T_s}{M}\right]^{0.5}\right)\left\{\frac{2}{n+1}\right\}H \quad \text{bar}, \tag{2}$$

where (in cgs units): R is the (nominal) film thickness deposition rate in cm s^{-1}; f is the laser repetition rate – note that $R/f\Delta t$ is the actual thickness deposition rate per laser pulse; A is the measured hot spot area; l is the distance from target to monitor; r is the radius of the exposed area of the rate monitor crystal; Δt is the measured effective hot spot time; ρ is the density of the film; M is the average gram molecular weight of the depositing species; R_g is the gas constant; $H = (1-0.18)^{-1}(2\pi/e)^{-0.5}$ and contains factors for relatively small hydrodynamic back-scattering and beam intensifying effects discussed elsewhere [6].

In earlier work, temperature T_s was obtained from a gas dynamic relationship between T_b, the post-expansion temperature (obtained from velocity distribution analysis) and T_s [5]. In the present work,

$$I(\lambda, T_s) = A\lambda^{-5}\left[e^{(c_2/\lambda T_s)} - 1\right]^{-1} \tag{3}$$

a direct measure was obtained using the wavelength distribution of light, $I(\lambda, T_s)$, emitted from the hot spot, according to the Planck radiation relation for grey or black body conditions: where A and C_2 are constants. Fig. 2 shows a typical result.

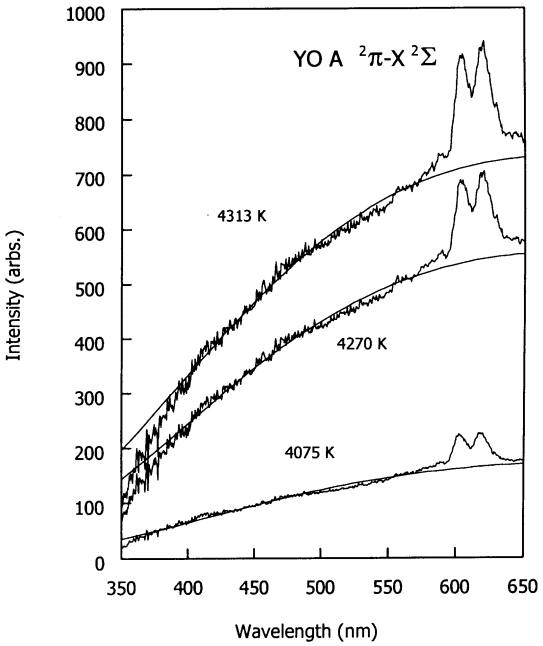

Fig. 2. Y_2O_3 temperature measurements based on Planck model fits (smooth curves) to emission versus wavelength. The peaks (ignored in fits) above 575 nm are known spectral transitions for YO.

3. Results

The new experimental approaches developed have been tested by comparison of measured partial and total pressures with reasonably well-established literature data for C and Al_2O_3. Table 2 shows representative comparisons for C.

Table 2
Partial pressure data comparisons with literature for C at 4100 K

Species[a]	P_i (this work)[b]	P_i [7]	P_i [8]
C_1	0.12	0.10	0.10
C_2	0.26	0.15	0.18
C_3	1.3	0.83	1.45
C_4	0.04	0.11	0.05
C_5	0.07	0.02	0.29

[a] C_6–C_9 also observed, but at negligible partial pressures.
[b] Uncertainities ± 30%, compared with factor of 4 [7] and factor of 5 [8].

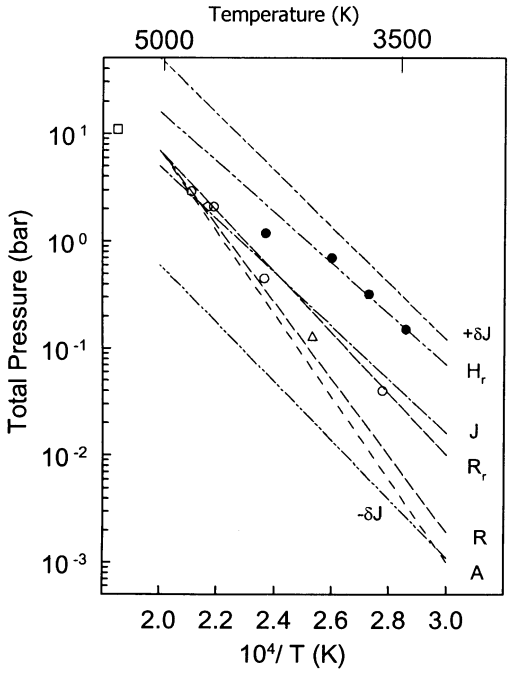

Fig. 3. Comparison of ZrO_2–7% Y_2O_3 P_t versus T data with extrapolated literature values (curves) – open symbols are for separate runs with unreduced (i.e. initial) material and closed symbols are for the partially reduced system (see text). Data uncertainty limits are similar to those indicated in Fig. 4. Curve R [8]; curve J [7], $\pm\delta J$ uncertainty; curve H_r extrapolation of Hoch et al. [10], $ZrO_2(s) + Zr(s)$ system; curve R_r calculated from [8] for $ZrO_2(\ell) + Zr(\ell)$ system; Curve A, extrapolation of Ackerman et al. [9] data for vaporization to $ZrO_2(g)$.

3.1. ZrO_2–7%Y_2O_3

Mass spectral analysis indicates ZrO, ZrO_2 and O as the main vapor species. Fig. 3 shows representative P_t data. From the lower temperature work of Ackerman et al. [9], ZrO_2 reduces with time by non-congruent vaporization. This behavior was also noted in the present work in the form of an enhanced vaporization rate with time, i.e., with successive laser shots. The results are consistent with the JANAF [7] evaluation for ZrO_2 and with the Hoch et al. [10] data for reduced ZrO_2.

3.2. Y_2O_3

The Y_2O_3 system is relatively simple, and well-behaved. The main species are YO and O, and negligible reduction occurs. Accordingly, the data, in Fig. 4, exhibit good precision. The results are consistent with the extrapolated values of Ames et al. [12].

3.3. HfO_2

The very few prior studies for HfO_2 have been evaluated by Schick [13] to yield the curves given in Fig. 5,

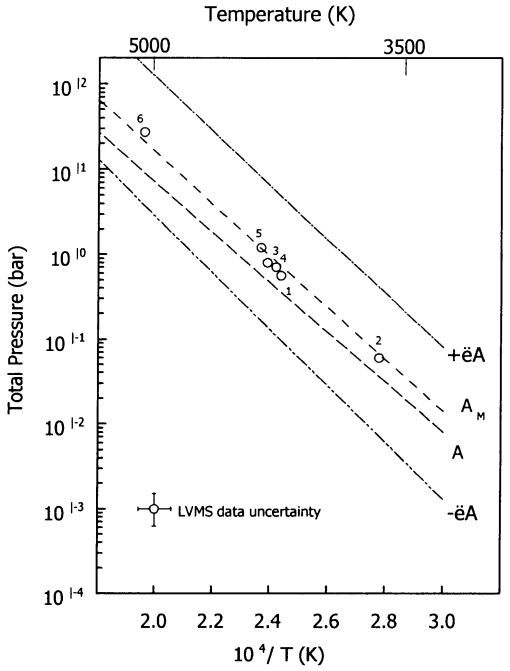

Fig. 4. Comparison of $Y_2O_3P_t$ versus T data with extrapolated literature values (curves). Data points (open circles) are numbered in chronological order. Curve A is extrapolated from solid phase data of Ackerman et al. [11] with an estimated enthalpy of melting; $\pm\delta A$ are uncertainties of [11]; curve A_M is extrapolated from Ames et al. [12].

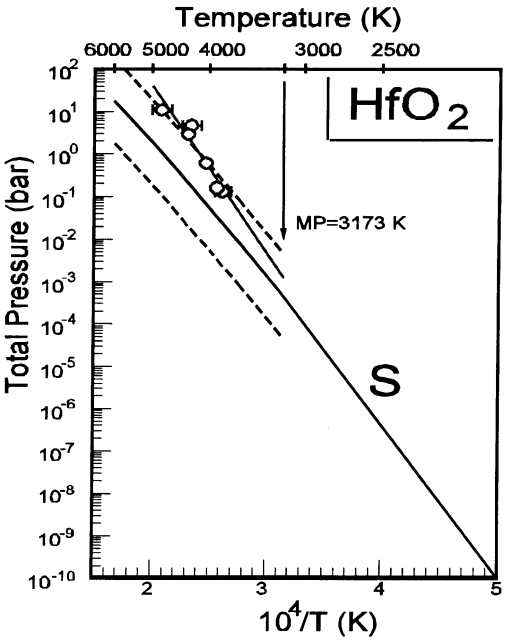

Fig. 5. Comparison of HfO_2 P_t versus T data (open circles) with extrapolated literature values (curve S) of Schick [13]). Dashed curves represent our estimated uncertainty range ± 10 in P_t values for the liquid region data from [13]. Size of error bars are indicative of assessed uncertainties in the present data.

together with results of the present work. HfO and O are the main species.

4. Summary and conclusions

The application of short-pulse laser heating to studies of thermal equilibrium vaporization processes has been demonstrated. Development of a direct approach to temperature and pressure measurement, on a nanosecond time-scale, now allows for relatively accurate thermochemical data to be obtained for nuclear and other refractory materials over the previously inaccessible ranges of 3000–5000 K and 10^{-4}–10 bar.

References

[1] R.W. Ohse, J.F. Babelot, C. Cercignani, J.P. Hiernout, M. Hoch, G.J. Hyland, J. Magill, J. Nucl. Mater. 130 (1985) 165.
[2] D.R. Olander, S.K. Yagnik, C.H. Tsai, J. Appl. Phys. 64 (1988) 2680.
[3] J.W. Hastie, D.W. Bonnell, P.K. Schenck, Molecular Basis for Laser-Induced Vaporization of Refractory Materials, NBSIR 84-2983, NTIS, Washington, DC, 1984.
[4] M. Joseph, N. Sivakumar, D. Darwin Albert Raj, C.K. Mathews, Rapid Commun. Mass Spectrom. 10 (1996) 5.
[5] J.W. Hastie, D.W. Bonnell, A.J. Paul, J. Yeheskel, P.K. Schenck, High Temp. Sci. 33 (1995) 135.
[6] J.W. Hastie, D.W. Bonnell, P.K. Schenck, Proc. 10th Int. IUPAC Conf. High Temp. Mater. Chem. 10–14 April, 2000, Julich, Germany, 2000.
[7] M.W. Chase Jr., C.A. Davies, J.R. Downey Jr., D.J. Frurip, R.A. McDonald, A.N. Syverud. JANAF Thermochemical Tables, 3rd Ed., J. Phys. Chem. Ref. Data 14, Suppl. No. 1, ACS, Washington, DC, 1985.
[8] L.V. Gurvich, I.V. Veyts, C.B. Alcock, Thermochemical Properties of Individual Substances, 4th Ed., Vols. 1–3., Hemisphere, New York, 1989 (Also, see original Russian editions loc. cit., and NIST Special Database 5, 'IVTANTHERMO' (L.V. Gurvich, V.S. Iorish, D.V. Chekhovsioi, V.S. Yungman, CRC, Boca Raton, FL 1993) – a program that incorporates the above tabulations to $\sim$ 1992, and can compute multicomponent equilibria using the database).
[9] R.J. Ackermann, E.G. Rauh, C.A. Alexander, High Temp. Science 7 (1975) 304.
[10] M. Hoch, M. Nakata, H.L. Johnston, J. Amer. Chem. Soc. 76 (1954) 2651.
[11] R.J. Ackermann, E.G. Rauh, R.J. Thorn, J. Chem. Phys. 40 (1964) 883.
[12] L.L. Ames, P.N. Walsh, O. White, J. Phys. Chem. 71 (1967) 2707.
[13] H.L. Schick, Thermodynamics of Certain Refractory Compounds, Vol. 1, Academic, New York, 1966.